PHYSICAL DRIVERS OF THE 2013 MARINE HEATWAVE IN THE SEAS OF THE SOUTHERN JAVA-NUSA TENGGARA

***Tria MAULIDA*[1,4], *Anindya WIRASATRIYA*[2,3], *Dwi Haryo ISMUNARTI*[2] *and Ardiansyah Desmont PURYAJATI*[2]**

DOI: 10.21163/GT_2022.171.10

ABSTRACT:
Marine heatwave (MHW) is an extreme phenomenon of warm sea surface temperature anomaly that has a destructive impact on the marine ecosystem and organisms. This phenomenon increases every year in duration, frequency, and area due to the global warming. Almost all of the world's oceans have experienced MHW, including in the seas of the southern Java-Nusa Tenggara. The lack of detailed research in this area motivated us to analyze MHW drivers. MHW was identified with the 99th percentile method and duration of ≥ 5 days as a threshold by using blended product of SST data. In 2013, an MHW event was identified in the seas of the southern Java-Nusa Tenggara. This MHW lasts for 37 days, from 8 June to 14 July. The maximum (mean) intensity of sea surface temperature anomaly reaches 2.60˚C (1.83˚C) above climatology with an average area of 36.53×10^4 km^2. Locally, we found that probably the positive downward shortwave radiation affected this anomaly. Furthermore, a remote process of the propagation of downwelling Kelvin wave during negative Indian Ocean Dipole may also affect this anomaly. The strong westerly wind along the equatorial Indian ocean forms downwelling Kelvin wave that propagates to the southern Java-Nusa Tenggara increasing SST in this area.

Key-words: *Marine heatwave, Extreme Sea surface temperature, Downwelling Kelvin wave, Remote Sensing, South Java-Nusa Tenggara*

1. INTRODUCTION

Global warming has increased the temperature of the earth's surface. This has also contributed to rising sea surface temperatures (SSTs)as the oceans have absorbed more than 93% of heat excess from greenhouse gas emissions since the 1970s (Rhein et al. 2013). It is noted that the global average SST has increased since the early 20th century and 1950. The average SST in the Indian, Atlantic and Pacific Oceans increased by 0.65˚C, 0.41˚C, and 0. 31˚C during the period 1950–2009. This SST increase results in more frequent extreme events and a greater risk to marine ecosystems (Hoegh-Guldberg et al. 2014). One category of extreme event that has attracted more attention from researchers is the Marine Heatwave (MHW).

MHW is a warm SST anomalous event that occurs for five days or more with an SST warmer than the 90th percentile based on a historical baseline period of 30 years (Hobday et al. 2016). MHW can also be defined by the relative threshold of the 99th percentile (Collins et al. 2019). Oliver et al. (2018) stated that the frequency, duration, and days of global MHW during 1925-2016 had increased

[1]*Faculty of Fisheries and Marine Sciences, Diponegoro University, 50275, Semarang, Indonesia, triamaulida2008@gmail.com*
[2]*Department of Oceanography, Faculty of Fisheries and Marine Sciences, Diponegoro University, 50275, Semarang, Indonesia, aninosi@yahoo.co.id, dwiharyois@lecturer.undip.ac.id, a.desmont213@gmail.com*
[3]*Center for Coastal Rehabilitation and Disaster Mitigation Studies, Diponegoro University, 50275, Semarang, Indonesia*
[4]*Indonesian Agency for Meteorology Climatology and Geophysics, 10610, Jakarta, Indonesia*

by 34%, 17%, and 54%, respectively. This trend of increasing MHW can undoubtedly continue to increase across the oceans as long as global warming continues.

Previous research has shown that many MHW events have occurred in oceans. Some of them are Western Australia 2010/2011 MHW (Pearce et al. 2011), the Atlantic Northwest 2012 MHW (Mills et al. 2013), the Northeast Pacific "The Blob" 2015 MHW (Bond et al. 2015), the Tasman Sea 2015 MHW (Oliver et al. 2017), and the North Pacific 2019 MHW (Amaya et al. 2020). The Indonesian Ocean was not spared from the MHW incident. Benthuysen et al. (2018) and Iskandar et al. (2021) showed the presence of MHW in the Indo-Australian Basin (9˚S to 18˚S, 110˚E to 122˚E) in 2016, and Ismail (2021) identified MHW in coastal and offshore areas of West Sumatra.

MHW in several oceans has a driver mechanism that varies significantly from region to region and is different in each case. MHW can generally occur due to atmospheric-ocean interactions, atmospheric conditions, ocean conditions, modulation of climate variability (MJO, ENSO, IOD, PDO), and remote teleconnection (Holbrook et al. 2020). For example, Pearce and Feng (2013) mention that the West Australia 2011 MHW occurred simultaneously as a strong La Niña, which increased the Leeuwin current and the presence of high-value air-to-ocean heat fluxes. The North Australian 2016 MHW, which included the Indo-Australian Basin, was due to a strong El Niño, which weakened monsoon activity resulting in a positive anomaly of heat flux entering the ocean (Benthuysen et al. 2018). The Northwest Atlantic 2015/2016 MHW occurred due to a combination of atmospheric-ocean processes, namely the position of the jet stream and ocean advection that played a role in heating the SST (Perez et al. 2021). The South Java MHW in 1998 and 2016 occurred due to the strong El Niño and weakening monsoons (Iskandar et al. 2021).

Research related to the mechanism that causes MHW has been proliferating throughout the world, but unfortunately, research related to this is still very lacking in the territory of Indonesia. Meanwhile, MHW can cause significant damage to marine organisms and ecosystems, such as the Northwest Atlantic 2012 MHW. This MHW disrupted fishery production, species shift, and low ocean productivity, so it impacted the socioeconomic (Mills et al. 2013). Another massive impact of MHW is causing coral bleaching, such as in the Bay of Bengal (Krishnan et al. 2011) to resistant corals in Western Australia (Le Nohaïc et al. 2017). Therefore, we are interested in conducting an analysis related to the causes of MHW in Indonesia's territory, namely the seas of the southern Java-Nusa Tenggara (**Fig. 1**).

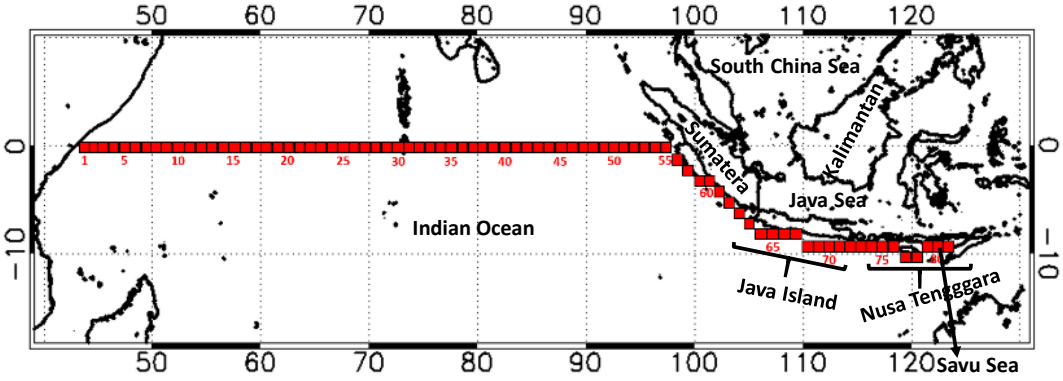

Fig. 1. Kelvin wave trajectory identified from the Indian Ocean to the coasts of Sumatra, Java, and Nusa Tenggara. The red box showed 81 sample areas with 0.1˚ × 0.1˚ bin sizes.

This location was chosen because the southern seas of Java-Nusa Tenggara are included in the State Fisheries Management Area of the Republic of Indonesia 573, which has excellent fishery potential. So that the analysis of the physical mechanisms of MHW and the extent to which local and remote factors play a role will improve our understanding of the development of MHW in this area.

Thus, this study can be a consideration in mitigating the impact to marine ecosystems if MHW retakes place.

2. DATA AND METHODS

Sea surface temperature data use daily Optimum Interpolation Sea Surface Temperature from Remote Sensing System (REMSS OISST) from June 2002-June 2021 with a resolution of 0.09˚ (ftp://ftp.remss.com/sst/daily/). This data uses microwave and infrared sensors. The microwave sensors used include the Global Precipitation Measurement (GPM) Microwave Imager (GMI), Tropical Rainfall Measuring Mission (TRMM) Microwave Imager (TMI), NASA Advanced Microwave Scanning Radiometer-EOS (AMSRE), Advanced Microwave Scanning Radiometer 2 (AMSR2), and WindSat. As for infrared sensors such as Moderate Resolution Imaging Spectroradiometer (MODIS) and Visible Infrared Imaging Radiometer Suite (VIIRS).

Sea level anomaly (SLA) data was obtained from https://resources.marine.copernicus.eu/products. This data is calculated by the optimal interpolation method and combines many data from various satellites such as Jason-3, Sentinel-3A, HY-2A, Saral/AltiKa, Cryosat-2, Jason-2, Jason-1, T/P, ENVISAT, GFO, ERS1/2. Monthly SLA data (SEALEVEL_GLO_PHY_L4_REP_OBSERVATIONS_008_047) with a resolution of 0.25˚ x 0.25˚ were used for the analysis and Hovmöller plots of the 2013 MHW.

The surface wind vector data used is the second version of the Cross-Calibrated Multi-Platform (CCMP) level 3 data. The second version of this data combines the wind speed RSS Radiometer version 7, QuikSCAT and the ASCAT wind vector scatterometer, tethered buoy wind data, and the ERA-Interim model. The compilation of this data was processed using the Variational Analysis Method (VAM). This method produces wind data with a high resolution of 0.25˚ with a data period of 6 hours, which can be downloaded via ftp://ftp.remss.com/ccmp.

The latent heat flux, sensible heat flux, and shortwave radiation data used are model data from ERA-5, a reanalysis product from the European Center for Medium-Range Weather Forecasts (ECMWF). These data were collected from January-December 2013 with 0.25˚ × 0.25˚ resolution available at https://cds.climate.copernicus.eu/cdsapp#!/dataset/reanalysis-era5-single-levels?tab=form. The coverage area used is 6˚S to 18˚S, 104˚E to 128˚E. Based on the ECMWF convention, these three data values are positive downwards. Positive downward means a positive value indicating the presence of heat or radiation entering the ocean. Conversely, a negative value indicates heat or radiation coming out of the ocean.

MHW identification was carried out by following Hobday et al. (2016), using a duration threshold of 5 days. However, we did not use the 90th percentile in this study but used the 99th percentile (Frölicher et al. 2018; Collins et al. 2019). The 99th percentile was chosen because this method identifies more extreme MHWs, so relatively weak MHWs and those that may not have an ecological impact can be eliminated. Besides that, this threshold value has never been applied in our research area.

Using Hobday et al. (2016), climatological averages (T_m) and threshold values (T_{99}) were calculated for each day of the year using the daily temperature data for each year. The equation for climatological averages (T_m) is expressed as follows:

$$T_m(j) = \sum_{y=y_s}^{y_e} \sum_{d=j-5}^{j+5} \frac{T(y,d)}{11(y_e - y_s + 1)} \quad (1)$$

where j is day of year, y_s and y_e are the start and end of the climatological base period, respectively, and T is the daily SST on day d and year y. T_m unit is °C.

As for the threshold, it is calculated based on

$$T_{99}(j) = P_{99}(X) \quad (2)$$

where T_{99} is the seasonally varying temperature value at the 99th percentile, P_{99} is the 99th percentile and $P_{99}(X)$ where $X = \{T(y,d)|y_s <= y <= y_e, j-5 <= d <= j+5\}$.

The period for calculating climatological value was limited only from 19 years data since REMSS OISST data is only available from June 2002. We chose REMSS OISST due to its high spatial resolution (i.e., 0.09°C) since our study area is limited only in the seas of the southern Java-Nusa Tenggara. Furthermore, Schlegel et al. (2019) stated that the detection of MHW can use time-series data less than 30 years, whereas the result of the short period analysis of 10 years does not have a duration or intensity of MHW that is sufficiently different from the events detected in the standard 30-year time series data as suggested by Hobday et al. (2016).

After the MHW was identified, we calculated the MHW metrics. The MHW metrics consist of duration (time between the start and end of the MHW event), maximum intensity (highest SST anomaly during MHW), average intensity (mean SST anomaly during MHW), and area size (areas where MHW was detected). To determine the parameters of duration (D), we must set the date on which MHW starts (t_s), where t_s is the time, t, where $T(t) > T_{99}(j)$ and $T(t-1) < T_{99}(j)$ and MHW ends (t_e), where t_e is the time, t, where $t_e > t_s$ dan $T(t) < T_{99}(j)$ and $T(t-1) > T_{99}(j)$, so the duration can be calculated using the formula

$$D = t_e - t_s \tag{3}$$

As for maximum intensity (i_{max}) and average intensity (i_{mean}), we use these equations:

$$i_{max} = \max(T(t) - T_m(j)) \tag{4}$$

$$i_{mean} = \overline{T(t) - T_m(j)} \tag{5}$$

For the analysis of the MHW trigger mechanism, Holbrook et al. (2020) mention that various mechanisms can trigger the occurrence of MHW. Locally, atmosphere-ocean interactions such as heat flux exchange can lead to an increase in SST. So, we will be analyzed the mechanism from local influences with parameters of wind speed, latent heat flux, sensible heat flux, and shortwave radiation. Besides that, we also analyze the SLA and zonal wind anomalies to determine the effect of Kelvin waves. To further investigate how Kelvin waves occur and their effect on SST, we construct a Hovmöller plot. The plot consists three parameters: SST, zonal wind anomalies, and SLA according to the Kelvin wave trajectory from the Indian Ocean to the coasts of Sumatra, Java and Nusa Tenggara as shown in **Fig. 1**. Analysis was also carried out in temporal variation using a coverage area of 8˚S to 9˚S, 112˚E to 115˚E (black box in **Fig. 2**).

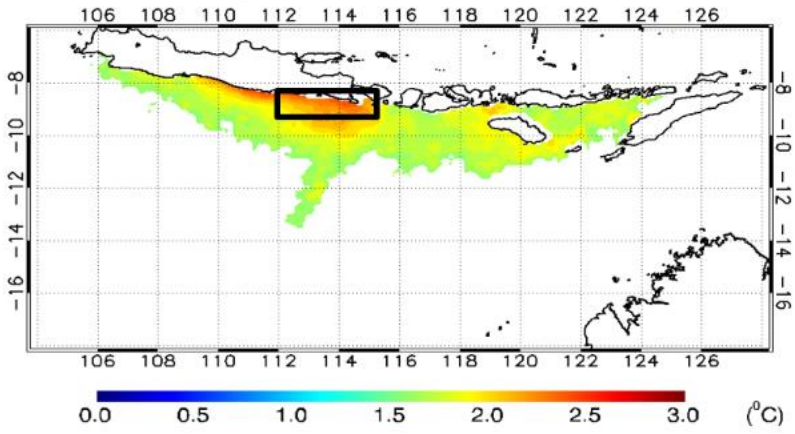

Fig. 2. MHW amplitude map for 8 June to 14 July. The colour bar shows the SST anomaly from the MHW threshold (smoothed daily climatology + 1.6˚C).

3. RESULTS AND DISCUSSION

3.1. Characteristic of 2013 MHW

Applying the method of Hobday et al. (2016) and Collins et al. (2019), we found a threshold value of SST anomaly to identify MHW is 1.6˚C. From this threshold value, 20 MHW events were identified during June 2002-June 2021. One of the longest cases was MHW in 2013 that occurred from 8 June to 14 July. We chose 2013 MHW as our case study because this MHW has a duration of more than one month. Based on the MHW metric parameters, the 2013 MHW had a duration of 37 days, a maximum intensity of 2.60˚C, the average intensity of 1.93˚C, and an area of 36.53×10^4 km^2.

Fig. 2 shows the 2013 MHW amplitude map. The 2013 MHW occurs in the southern coast of Java to Nusa Tenggara. The highest SST anomaly value occurs in the southern coast of Java, precisely in the southern coast of East Java, with an anomaly value of 2.75˚C. In general, the value of the SST anomaly is higher in the coastal seas i.e., about 2.5˚C than off the coast, where the value decreases to 1.6˚C. Ismail (2021) also showed that the 1998 and 2016 MHWs that occurred in the west coast of Sumatra had a more severe category, than the offshore area, which was only detected in the moderate to strong category. High SST values in the coastal seas can occur due to various factors. Coastal areas where land, sea, and air meet have complex SST variation mechanisms (Wirasatriya et al. 2019a).

Next, we made the temporal variation of SST with the threshold value and the climatological mean (**Fig. 3**). Temporal variation of SST was averaged from the area with the highest anomaly value, i.e., 8˚S to 9˚S, 112˚E to 115˚E (black box in **Fig. 2**). Red shading indicates the period of identified MHW. **Fig. 3a** shows the variation of SST during 2013 and we identified one MHW incident which is categorized as an extreme event. The temporal variation of SST during the 2013 MHW event (**Fig. 3b**) shows that the SST value exceeds the 99th percentile threshold from 8 June with an SST value of 29.19˚C. The SST value in this incident ranges from 29.37 to 27.55˚C. On 10 July, the SST value starts to decline, approaches the threshold value, and finally ends on 14 July with an SST value of 27.55˚C.

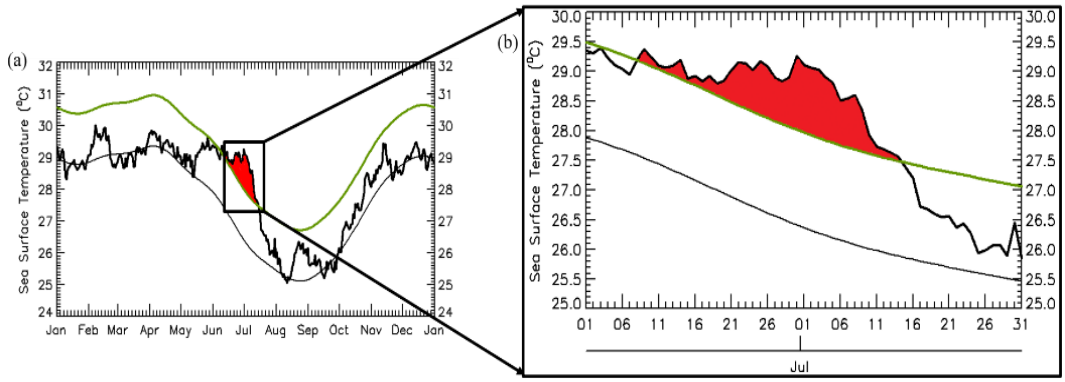

Fig. 3. Temporal variation of SST (thick black line), SST climatology (thin black line) and 99th percentile climatology (green line) during (a) 2013 and (b) 2013 MHW events at 8˚S to 9˚S, 112˚E to 115˚E (black box in Fig. 2). The red shaded indicates the occurrence of MHW.

In addition, we also compared the SST anomaly with the area during MHW 2013 (**Fig. 4**). At the beginning of its occurrence, MHW has an area of 5.19×10^4 km^2 with an SST anomaly of 1.61˚C. The area of MHW increases along with the increasing value of the SST anomaly. However, at the highest SST anomaly, which occurs on 14 July (2.75˚C), the previous maximum area occurs on 28 June at 25.66×10^4 km^2. Meanwhile, at the end of the MHW period, the area is getting smaller and ends up with 7.52×10^4 km^2.

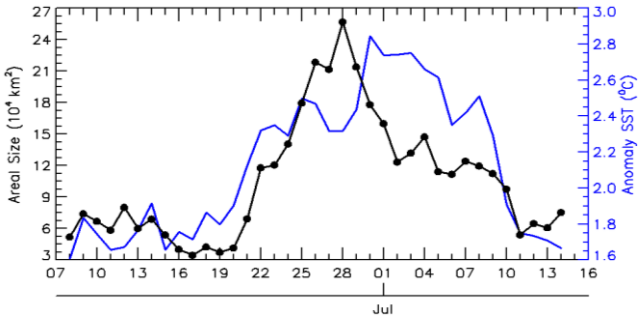

Fig. 4. Temporal variation of MHW area (black line) with SST anomaly (blue line) during MHW 2013.

3.2. Mechanisms of 2013 MHW

During 2013 MHW, the wind blows from the east-southeast direction (**Fig. 5a**). The wind speed in the southern coast of Java-Nusa Tenggara ranges from 2 to 6 m/s. This is lower than the offshore wind speed which is ranging from 6 to 8 m/s. Theoretically, the wind speed variation can affect the latent heat flux. For example, Wirasatriya et al. (2019b) stated that the increase in wind speed in the Sulawesi Sea and the Maluku Sea increases the latent heat flux released from the ocean. In the present study the latent heat flux distribution during 2013 MHW is shown in **Fig. 5b**.

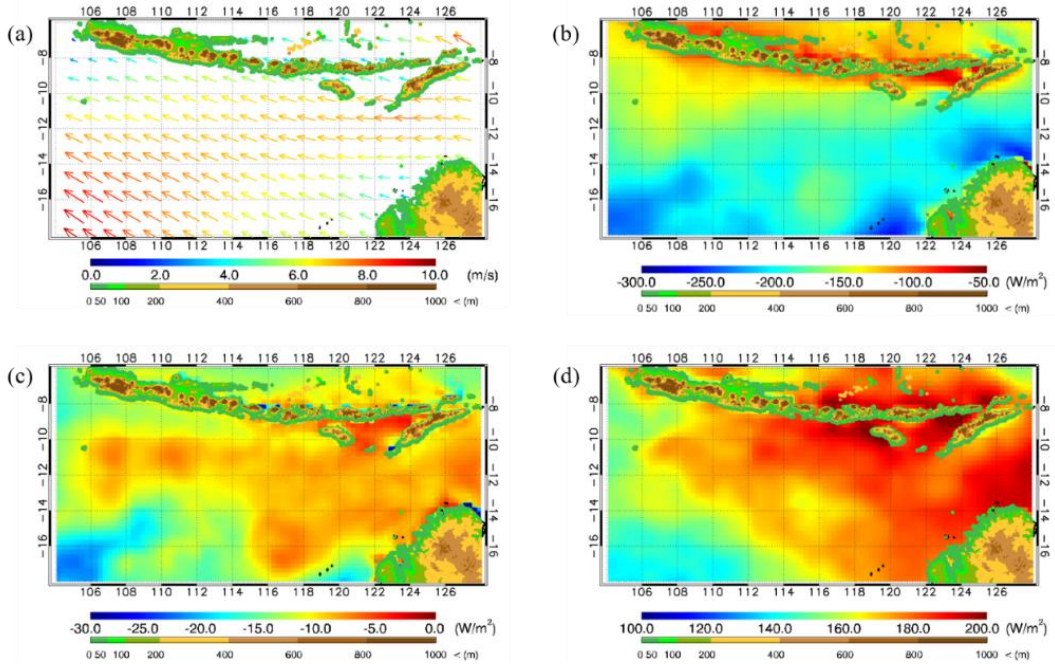

Fig. 5. Spatial distribution of (a) surface wind, (b) latent heat flux, (c) sensible heat flux, and (d) shortwave radiation during 2013 MHW.

Negative values of latent heat flux dominate the entire MHW area. This negative value indicates that the oceans are losing heat due to the heat escaping. The southern coast of Java-Nusa Tenggara, which has lower wind speeds, tends to release a lower latent heat flux (i.e., -50 to -150 W/m2) than the offshore area. Meanwhile, offshore area with higher wind speed releases more significant heat flux, i.e., -150 to -200 W/m^2.

The distribution of negative values is also visible for the sensible heat flux distribution (**Fig. 5c**). There is no difference between coastal and offshore in the sensible heat flux. This flux value ranges from 0 to -15 W/m^2. The lowest sensible heat flux is detected in the Savu Sea which ranges from 0 to -5 W/m^2. The lowest value indicates that the air temperature in the Savu Sea is lower than in other ocean areas. This results in less heat loss compared to other areas. However, compared with the MHW amplitude map (**Fig. 2**), the less heat loss in the Savu Sea does not have a significant effect because the SST anomaly value is only around 1.7˚C.

In contrast to the latent and sensible heat flux, the shortwave radiation shows a positive distribution of values (**Fig. 5d**). The value of shortwave radiation on the coast of the island to the offshore is relatively the same as the value of 170-200 W/m^2. Areas with >200 W/m^2 generally occur in the south of West Nusa Tenggara and the Savu Sea. Meanwhile, in other areas with less than 200 W/m^2, including the southern region of East Java has the highest SST anomaly value. This positive value indicates that there is a radiation entering the sea which can heating the SST. In the case of South Atlantic, 2013/2014 MHW occurred because of the increase of shortwave radiation intensity due to the reduced cloud cover and reduced heat loss from the ocean (Rodrigues et al. 2019).

Since the analysis of heat flux and wind speed could not explain well the mechanism of MHW 2013, we analyzed the possible contribution of remote modulation such as Kelvin wave propagation. Tracking Kelvin waves eastward along the equator and then along the coasts of Sumatra and Java can be done effectively using altimetry satellites (Drushka et al. 2010). Kelvin wave propagation can be observed using SLA data. We can determine whether the Kelvin wave is downwelling or upwelling from the SLA data.

The Hovmöller SST diagram (**Fig. 6a**) shows several SST anomalies that exceed the threshold value of the 99th percentile as in June-July and August. However, the most extensive and most widespread anomaly occurred from 8 June to 14 July. The SST anomaly value was detected from bin 64-81, i.e., the Southern coat of Java-Nusa Tenggara area. As for the Hovmöller diagram of the zonal wind anomaly during 2013 (**Fig. 6b**), bin 64-81 (south of Java-Nusa Tenggara) has a negative value, indicating an easterly wind occurrence. From this anomaly, it is known that the easterly wind is stronger than the climatological value.

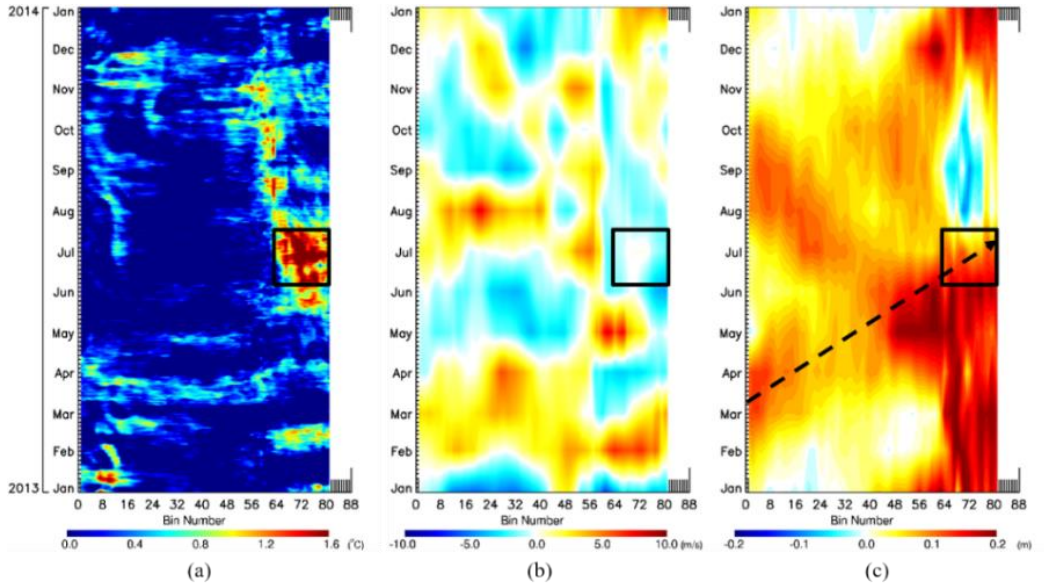

Fig. 6. Hovmöller diagram (a) SST, (b) zonal wind anomaly, and (c) SLA in 2013. Bin 1-55 shows the Indian Ocean region, bin 56-62 the coastal area of Sumatra, and bin 63-81 the coastal area of Java -Nusa Tenggara. The dashed black arrow in fig. c shows the direction of the downwelling Kelvin wave propagation. The black box indicates the 2013 MHW period.

Easterly wind anomaly generally causes upwelling Kelvin wave that cools SST (Drushka et al. 2010). However, in the southern region of Java to Nusa Tenggara, the MHW has a hot SST anomaly. We suspect that the SST warm anomaly is caused by a long-distance process, namely the downwelling Kelvin wave propagation. From April to October (**Fig. 7,** red line), a negative Indian Ocean Dipole (IOD) value is detected. A negative IOD causes an increase in westerly winds blowing along the equator of the Indian Ocean so that it can trigger a downwelling Kelvin wave (**Fig. 8b**). Although the IOD value had started to return to normal at the MHW incident, the propagation of the downwelling Kelvin wave is still going on and affects the southern Java-Nusa Tenggara region. This may cause an increase of the SST anomaly in the area.

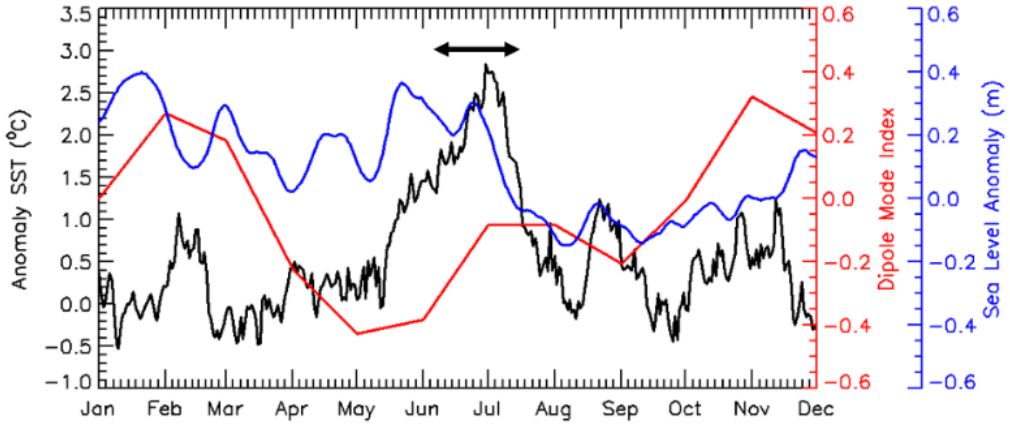

Fig. 7. Temporal variation between SST anomalies (black line) at 8˚S to 9˚S, 112˚E to 115˚E (black box in Fig. 2) with Dipole Mode Index (DMI) (red line) and SLA (blue line) during 2013. The black arrow shows the 2013 MHW period.

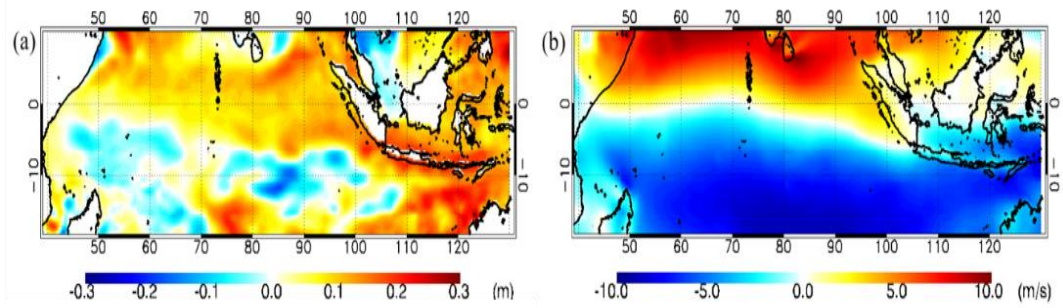

Fig. 8. Amplitude map of (a) SLA and (b) zonal wind during 2013 MHW.

The indication of the downwelling Kelvin wave is depicted on the Hovmöller SLA diagram (**Fig. 6c**). Positive SLA values are identified from bin 1 to 88 during March-August. The highest positive value >0.2 m occurred in April-June at bin 48-70, i.e., from the central Indian Ocean region to the southern coast of Java. Meanwhile, for the coastal areas of Java-Nusa Tenggara (bin 64-81), the positive SLA value is consistently seen from January to the end of August.

In addition, the SLA time series (**Fig. 7**, blue line) shows consistent positive values during the 2013 MHW period. The highest SLA values reach up to 0.3 m on 24-25 June, and as MHW end, the SLA values decrease to -0.03 m. From the SLA map during 2013 MHW (**Fig. 8a**), positive SLA values are distributed throughout the MHW area, both inshore and offshore areas. The value of SLA on the coast ranges from 0.2 to 0.3 m, higher than the SLA in the offshore, which has a value of 0.1-0.2 m.

The positive SLA value up to 0.3 m indicates the downwelling Kelvin wave and is the dominant mechanism in causing 2013 MHW. Based on Kutsuwada and McPhaden (2002), downwelling Kelvin wave can suppress the thermocline by several meters, raising sea level elevation by several centimeters and increasing the SST above the thermocline. As happened in Northern Australia, the propagation of sea Kelvin waves triggered by La Niña causes the warm SST anomaly (Benthuysen et al. 2014). In addition, the Kelvin wave also affected the phenomenon of warm SST on the coast of Angola-Namibia in 1995, known as the Benguela Niño. These Kelvin waves are triggered by Atlantic tropical wind anomalies (Gammelsrød et al. 1998). On the other hand, a negative SLA value indicates the upwelling Kelvin wave because the upwelling Kelvin wave propagation induces a negative SLA anomaly along the southern coast of Sumatra-Java (Li et al. 2018).

From these results, we found that the propagation of the downwelling Kelvin wave is one of the driving mechanisms that caused the 2013 MHW in Southern Java-Nusa Tenggara besides the shortwave radiation. However, it should be noted that this is case study research so that the mechanism obtained only applies to the case of the 2013 MHW event and cannot be generalized for the other MHW cases. Each MHW event will have a different mechanism variation in each case, depending on the location and time of the incident. Holbrook et al. (2020) stated that the mechanisms that affect MHW vary greatly, influenced by local scales, large-scale modulation of climate variability or teleconnection mechanisms such as planetary wave propagation in the atmosphere or ocean. So, the mechanism of one MHW case cannot be generalized as the cause of another MHW case. As an example, the results of the driving mechanism for the 2013 MHW are different from the mechanism for 1998 and 2016 MHWs in Southern Java. Based on Iskandar et al. (2021), 1998 and 2016 MHW in South Java occurred in the austral winter months, lasted during the austral spring, disappeared in the early austral winter, and lived with intense El Niño events. During this El Niño period, the Australian monsoon weakens. These two things are most likely the cause of the 1998 and 2016 MHWs in South Java.

4. CONCLUSIONS

We have found MHW events in the seas of the southern Java-Nusa Tenggara in 2013, which occurs from 8 June to 14 July with an extreme category. The metric parameters of this MHW have duration, maximum intensity, average intensity, and area with values of 37 days, 2.60˚C, 1.83˚C, and 36.53×10^4 km^2, respectively. The highest anomaly value occurs on the southern coast of East Java at 2.75˚C. The SST warm anomaly occurs due to the downwelling Kelvin wave because of the westerly wind blowing along the equatorial Indian Ocean during the negative IOD. Downwelling Kelvin wave is identified from the positive value of SLA that occurred during the MHW incident. In addition, shortwave radiation may also play a role in increasing SST in Southern Java-Nusa Tenggara due to heat entering the ocean. Related mechanisms about MHW are an interesting subject for future studies, so further understanding of these MHW mechanisms is needed by adding large-scale climate variability analyses such as IOD, ENSO, and MJO.

ACKNOWLEDGEMENTS

The authors would like to thank you for the support from PUSDIKLAT BMKG and Diponegoro University. CCMP Version-2.0 vector wind analyses and REMSS OISST data are produced by Remote Sensing Systems available at www.remss.com. Sea level anomaly is provided by CMEMS available at https://resources.marine.copernicus.eu/products.

Latent heat flux, sensible heat flux, and shortwave radiation are provided by ERA5 available at https://cds.climate.copernicus.eu/cdsapp#!/dataset/reanalysis-era5-single-levels?tab=form.

REFERENCES

Amaya, D.J., Miller, A.J., Xie, S.P. and Kosaka, Y. (2020). Physical drivers of the summer 2019 North Pacific marine heatwave. *Nature Communications*, 11(1), pp.1–9. Available from: http://dx.doi.org/10.1038/s41467-020-15820-w.

Benthuysen, J., Feng, M. and Zhong, L. (2014). Spatial patterns of warming off Western Australia during the 2011 Ningaloo Niño: Quantifying impacts of remote and local forcing. *Continental Shelf Research*, 91, pp.232–246. Available from: http://dx.doi.org/10.1016/j.csr.2014.09.014.

Benthuysen, J.A., Oliver, E.C.J., Feng, M. and Marshall, A.G. (2018). Extreme Marine Warming Across Tropical Australia During Austral Summer 2015–2016. *Journal of Geophysical Research: Oceans*, 123(2), pp.1301–1326.

Bond, N.A., Cronin, M.F., Freeland, H. and Mantua, N. (2015). Causes and impacts of the 2014 warm anomaly in the NE Pacific. *Geophysical Research Letters*, 42(9), pp.3414–3420.

Collins, M., Sutherland, M., Bouwer, L., Cheong, S.-M., Frölicher, T., Jacot Des Combes, H., Koll Roxy, M., Losada, I., McInnes, K., Ratter, B., Rivera-Arriaga, E., Susanto, R. D., Swingedouw, D., and Tibig, L. (2019), Extremes, Abrupt Changes and Managing Risks, In: Pörtner, H.-O., Roberts, D. C., Masson-Delmotte, V., Zhai, P., Tignor, M., Poloczanska, E., Mintenbeck, K., Alegria, A., Nicolai, M., Okem, A., Petzold, J., Rama, B., and Weyer, N. M. (eds.) *IPCC Special Report on the Ocean and Cryosphere in a Changing Climate*, in press.

Drushka, K., Sprintall, J., Gille, S.T. and Brodjonegoro, I. (2010). Vertical structure of Kelvin waves in the Indonesian throughflow exit passages. *Journal of Physical Oceanography*, 40(9), pp.1965–1987.

Frölicher, T.L., Fischer, E.M. and Gruber, N. (2018). Marine heatwaves under global warming. *Nature*, 560(7718), pp.360–364.

Gammelsrød, T., Bartholomae, C.H., Boyer, D.C., Filipe, V.L.L. and O'Toole, M.J. (1998). Intrusion of warm surface water along the Angolan-Namibian coast in February-March 1995: The 1995 Benguela Nino. *South African Journal of Marine Science*, 7615(19), pp.41–56.

Hobday, A.J., Alexander, L. V., Perkins, S.E., Smale, D.A., Straub, S.C., Oliver, E.C.J., Benthuysen, J.A., Burrows, M.T., Donat, M.G., Feng, M., Holbrook, N.J., Moore, P.J., Scannell, H.A., Sen Gupta, A. and Wernberg, T. (2016). A hierarchical approach to defining marine heatwaves. *Progress in Oceanography*, 141, pp.227–238.

Hobday, A. J., Oliver, E. C., Sen Gupta, A., Benthuysen, J. A., Burrows, M. T., Donat, M. G., Holbrook, N. J., Moore, P. J., Thomsen, M. S., Wernberg, T., and Smale, D. A. (2018). Categorizing and naming marine heatwaves. *Oceanography*, 31(2), 162-173.

Hoegh-Guldberg, O., Cai, R., Poloczanska, E. S., Brewer, P. G., Sundby, S., Hilmi, K., Fabry, V. J., and Jung, S. (2014), The Ocean, In: Barros, V. R., Field, C. B., Dokken, D. J., Mastrandrea, M. D., Mach, K. J., Bilir, T. E., Chatterjee, M., Ebi, K. L., Estrada, Y. O., Genova, R. C., Girma, B., Kissel, E. S., Levy, A. N., MacCraken, S., Mastrandrea, P. R., and White, L. L. (eds.) *Climate Change 2014: Impact, Adaptation, and Vulnerability. Part B: Regional Aspects. Contribution of Working Group II to the Fifth Assessment Report of the Intergovernmental Panel on Climate Change*, Cambridge University Press, Cambridge, United Kingdom and New York, 1655-1731.

Holbrook, N.J., Sen Gupta, A., Oliver, E.C.J., Hobday, A.J., Benthuysen, J.A., Scannell, H.A., Smale, D.A. and Wernberg, T. (2020). Keeping pace with marine heatwaves. *Nature Reviews Earth and Environment*, 1(9), pp.482–493. Available from: http://dx.doi.org/10.1038/s43017-020-0068-4.

Iskandar, M.R., Ismail, M.F.A., Arifin, T. and Chandra, H. (2021). Marine heatwaves of sea surface temperature off south Java. *Heliyon*, 7(12).

Ismail, M.F.A. (2021). Characteristics of Marine Heatwaves off West Sumatra Derived from High-Resolution Satellite Data. *Journal of Hunan University Natural Sciences*, 48(6), pp.130–136.

Krishnan, A.P., Roy, S.D., George, G., Srivastava, R.C., Anand, A., Kaliyamoorthy, M., Vikas, N. and Soundararajan, R. (2011). Elevated sea surface temperature during May 2010 induces mass bleaching of corals in the Andaman Published by : Current Science Association Stable URL : http://www.jstor.org/stable/24069723 Elevated sea surface temperature duri. *Current Science*, 100(1), pp.111–117.

Kutsuwada, K. and McPhaden, M. (2002). Intraseasonal variations in the upper equatorial Pacific ocean prior to and during the 1997-98 El Niño. *Journal of Physical Oceanography*, 32(4), pp.1133–1149.

Li, S., Wei, Z., Susanto, R.D., Zhu, Y., Setiawan, A., Xu, T., Fan, B., Agustiadi, T., Trenggono, M. and Fang, G. (2018). Observations of intraseasonal variability in the Sunda Strait throughflow. *Journal of Oceanography*, 74(5), pp.541–547. Available from: https://doi.org/10.1007/s10872-018-0476-y.

Le Nohaïc, M., Ross, C.L., Cornwall, C.E., Comeau, S., Lowe, R., McCulloch, M.T. and Schoepf, V. (2017). Marine heatwave causes unprecedented regional mass bleaching of thermally resistant corals in northwestern Australia. *Scientific Reports*, 7(1), pp.1–11.

Mills, K. E., Pershing, A. J., Brown, C. J., Chen, Y., Chiang, F.-S., Holland, D. S., Lehuta, S., Nye, J. A., Sun, J. C., Thomas, A. C., and Wahle, R. A. (2013). Fisheries management in a changing climate: Lessons from the 2012 ocean heat wave in the Northwest Atlantic. *Oceanography*, 26(2), 191-195.

Oliver, E.C.J., Donat, M.G., Burrows, M.T., Moore, P.J., Smale, D.A., Alexander, L. V., Benthuysen, J.A., Feng, M., Sen Gupta, A., Hobday, A.J., Holbrook, N.J., Perkins-Kirkpatrick, S.E., Scannell, H.A., Straub, S.C. and Wernberg, T. (2018). Longer and more frequent marine heatwaves over the past century. *Nature Communications*, 9(1), pp.1–12. Available from: http://dx.doi.org/10.1038/s41467-018-03732-9.

Oliver, E.C.J., Benthuysen, J.A., Bindoff, N.L., Hobday, A.J., Holbrook, N.J., Mundy, C.N. and Perkins-Kirkpatrick, S.E. (2017). The unprecedented 2015/16 Tasman Sea marine heatwave. *Nature Communications*, 8(May), pp.1–12. Available from: http://dx.doi.org/10.1038/ncomms16101.

Pearce, a, Lenanton, R., Jackson, G., Moore, J., Feng, M. and Gaughan, D. (2011). *The "marine heat wave" off Western Australia during the summer of 2010/11. Fisheries Research Report No. 222. Department of Fisheries, Western Australia*.

Perez, E., Ryan, S., Andres, M., Gawarkiewicz, G., Ummenhofer, C.C., Bane, J. and Haines, S. (2021). Understanding physical drivers of the 2015/16 marine heatwaves in the Northwest Atlantic. *Scientific Reports*, 11(1), pp.1–11. Available from: https://doi.org/10.1038/s41598-021-97012-0.

Rhein, M., Rintoul, S. R., Aoki, S., Campos, E., Chambers, D., Feely, R. A., Gulev, S., Johnson, G. C., Josey, S. A., Kostianoy, A., Mauritzen, C., Roemmich, D., Talley, L. D., and Wang, F. (2013), Observation: Ocean, In: Stocker, T. F., Qin, D., Plattner, G-K., Tignor, M., Allen, S. K., Boschung, J., Nauels, A., Xia, Y., Bex, V., and Midgley, P. M. (eds.) *Climate change 2013: The Physical Science Basis Contribution of Working Group I to the Fifth Assessment Report of the Intergovernmental Panel on Climate Change*, Cambridge University Press, Cambridge, United Kingdom and New York.

Rodrigues, R.R., Taschetto, A.S., Sen Gupta, A. and Foltz, G.R. (2019). Common cause for severe droughts in South America and marine heatwaves in the South Atlantic. *Nature Geoscience*, 12(8), pp.620–626.

Schlegel, R.W., Oliver, E.C.J., Hobday, A.J. and Smit, A.J. (2019). Detecting Marine Heatwaves With Sub-Optimal Data. *Frontiers in Marine Science*, 6(November), pp.1–14.

Wirasatriya, A., Kawamura, H., Koch, M. and Helmi, M. (2019a). Satellite-borne detection of high diurnal amplitude of sea surface temperature in the seas west of the Tsugaru Strait, Japan, during Yamase wind season. *Journal of Oceanography*, 75(1), pp.23–36.

Wirasatriya, A., Sugianto, D.N., Helmi, M., Setiawan, R.Y. and Koch, M. (2019b). Distinct Characteristics of SST Variabilities in the Sulawesi Sea and the Northern Part of the Maluku Sea during the Southeast Monsoon. *IEEE Journal of Selected Topics in Applied Earth Observations and Remote Sensing*, 12(6), pp.1763–1770.